Performance Limitations of a Practical PCM Terminal

By R. H. SHENNUM and J. R. GRAY

(Manuscript received July 12, 1961)

This paper discusses the performance of a practical PCM terminal for time-division speech transmission. Limitations which make performance different from more conventional frequency-division systems are considered. Particular emphasis is placed on limitations resulting from nonideal circuits and signal conditions. Both analytical and experimental results are presented with comparisons given where appropriate.

I. INTRODUCTION

The limitations of frequency-division systems have been discussed in the literature. This paper treats the limitations of a practical PCM terminal which make its performance different from more conventional systems. The areas to be discussed include (1) signal deterioration due to noise and distortion, (2) idle circuit noise and interchannel crosstalk, (3) net loss and (4) load capacity. Analytical discussions are presented and compared with experimental results on models assembled at Bell Telephone Laboratories.

II. SIGNAL DETERIORATION DUE TO NOISE AND DISTORTION

The deliberate error imparted to the signal by quantization is the significant source of signal impairment in a PCM terminal. Other effects arising in a practical terminal also affect signal quality. The sections to follow consider both the quantizing impairment found in an "ideal" terminal,* and the tolerances required in the laboratory version to meet system signal-to-noise objectives. Signal-to-noise measurements over 24 channels are also provided and substantiate calculations and assumptions.

* The word "ideal" is used because it is found in the literature. In some instances the experimental terminal was designed intentionally to depart from the so-called "ideal" performance as will become evident later.

2.1 *Quantizing Noise*

Quantization is the process of converting the exact sample values of the signal to their nearest equivalent in a discrete set of amplitudes to permit digital encoding and, therefore, essentially noise-free transmission in the medium. The error or noise produced by this "rounding-off" procedure is the major source of signal impairment. The choice of quantization or coding function is governed by the statistics of the signal to be processed. For time-division speech channels, nonuniform quantization yields the best over-all signal-to-noise performance for a given bandwidth. To obtain comparable performance with uniform quantization would require an increase in sampling frequency and/or an increase in the number of quantizing levels for the same signal range. Both of these would result in an increase in bandwidth over nonuniform quantization.

Nonuniform quantization can be achieved directly by nonlinear encoding, or by first compressing the input signal and then applying uniform quantization. In the case of the latter, an instantaneous compressor network attempts to improve performance for weak signals by giving them preferential amplification. After encoding, transmission and decoding, a device called the expandor employing the inverse characteristic restores the proper quantized amplitude distribution. The two networks together are referred to as a compandor, and the signal-to-noise advantage for weak signals over that obtained with the simpler uniform quantization is the companding improvement. In the experimental system, a logarithmic compandor and a separate uniform encoder-decoder combination are used as discussed in a companion paper.[1]* Analytic treatment of the signal-to-noise behavior of a PCM terminal with this type of quantization has been covered in a paper by B. Smith.[2] His results for an input speech signal, assuming 7-digit encoding with 26-db logarithmic companding are reproduced in Fig. 1. These latter are the broad design parameters of the system.

2.2 *Departures from "Ideal" Performance*

The performance of the laboratory terminal deviates from the signal-to-noise behavior of Fig. 1. This is attributed to several causes. One source is the difference between the logarithmic compression characteristic derived from a practical diode network and the $\mu = 100$ curve discussed by Smith. The departure is in part intentional as a result of the desire to improve the signal-to-noise ratio at low signal amplitudes.

* Discussions of certain nonlinear encoding schemes are also included therein.

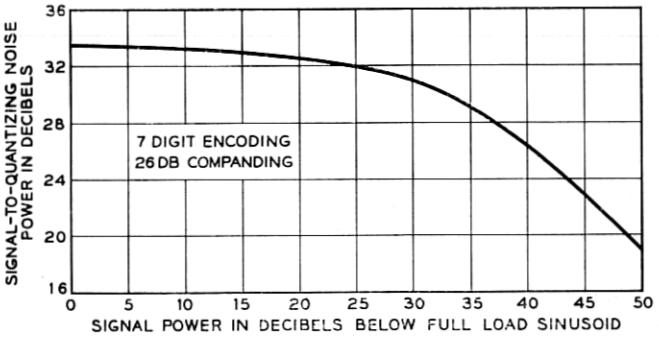

Fig. 1 — Plot of signal-to-quantizing noise as a function of signal level below full load sinusoid. Seven-digit encoding and 26-db companding are assumed.

At other values of the input signal, the diode network characteristic is constrained so that signal-to-noise ratios calculated with sinusoidal inputs using the experimental compression curve are a maximum of 3 db down at any point. The acceptance of a maximum penalty of 3 db is based on the fact that this maximum is confined to a relatively narrow signal range and on the existence of other ranges for which performance is better than shown in Fig. 1. This is shown elsewhere.[1]

Other major sources of imperfection are listed below. Each is assigned a margin such that the measured signal-to-noise performance is no more than 3 db lower than *calculated* performance as described above. These numbers assume that the contribution of each adds on a power basis to the theoretical quantizing impairment. They are also based on the fact that all do not degrade signal quality over the entire range of signal amplitudes:

(1) Encoder-decoder fine structure	1 db
(2) Pedestal variation prior to compression	2 db
(3) Compandor mistracking	1 db
(4) Encoder dc shift	1 db

In a practical encoder-decoder design, uniformity of step size and infinitely sharp transitions between adjacent quantized levels can only be realized approximately. An estimate of the effect of these imperfections on signal-to-noise behavior is calculated elsewhere.[1] Based on the margin assigned to code scale fine structure above, tolerances on the elements of the encoder and decoder networks are also given therein.

Pedestal variation is introduced at the multiplex gates as a result of sampling and causes misbiasing of the compressor network. The pre-

dominant effect in this case is a loss of companding improvement for weak signals as demonstrated by Smith.[2] Strong and midrange signals are relatively unaffected. The experimental system exhibits less of a degradation in this regard than predicted by Smith for $\mu = 100$ compandors. The reason for this is the greater range of linearity near the origin in the characteristics of the practical compandor networks. With a bias error at the compressor input of 1 per cent of the system overload voltage, approximately 2 db loss in companding improvement is found experimentally. This appears to be a realistic tolerance on pedestal variation, based on a desire for economy consistent with reasonable performance.

Compandor mistracking results when the transmission characteristics provided by the compressor and expandor networks are not exactly complementary. This introduces nonlinearities on through transmission. The primary effect is 3rd harmonic distortion as discussed by Mann, Straube, and Villars.[1] The 1-db margin allowed is based on the fact that only large signals are distorted. Weak signals are relatively unaffected since over-all linearity is maintained reasonably well in this range.

Besides 3rd harmonic distortion introduced by mistracking, 2nd harmonic distortion is also important. The outstanding contributor is unwanted dc reference drift at the coder, which in conjunction with companding results in a departure from linear transmission. To illustrate this effect, the transmission between compressor input and expandor output with an intermediate reference shift ϵ at the encoder is determined below.

Using the compression characteristic given by Smith, the compressor output is defined by*

$$\begin{aligned} y &= \frac{\log (1 + \mu x)}{\log (1 + \mu)} \qquad (0 \leqq x \leqq 1) \\ y &= \frac{-\log (1 - \mu x)}{\log (1 + \mu)} \qquad (-1 \leqq x \leqq 0) \end{aligned} \tag{1}$$

where μ is the compression parameter, and x is the input normalized to the compressor overload voltage. If quantization at the encoder is neglected, but its reference shifts by an amount ϵ, then the decoded output becomes $y + \epsilon$. Taking the expandor characteristic to be the inverse of the above, and assuming ϵ to be small and positive, then the expandor output as a function of the compressor input is approximately

* Unless otherwise specified, natural logarithms are implied.

$$F(x) \sim \alpha x \qquad (0 \leqq x \leqq 1)$$
$$F(x) \sim \frac{1}{\alpha} x \qquad (-1 \leqq x \leqq 0) \tag{2}$$

where $\alpha \sim 1 + \epsilon \log (1 + \mu)$. Equation (2) is illustrated by Fig. 2.

For a sinusoidal test signal of amplitude E at the compressor input, the expandor output would appear as a positive half-cycle sine wave with amplitude αE followed by a negative half-cycle of amplitude E/α. The 2nd harmonic content of such a wave is $-[(2/3\pi)E(\alpha^2 - 1/\alpha)]$ and the signal-to-2nd harmonic distortion becomes $| S/D | = 3\pi\alpha/2(\alpha^2 - 1)$. This result is plotted in Fig. 3, with ϵ given as a percentage of compressor overload voltage. In calculating this curve, μ is taken to be 100, corresponding approximately to the companding advantage obtained in the experimental system.

To meet the 1-db noise penalty assigned to this cause, coder reference drift must be restricted. The allowable drift is determined from the minimum acceptable signal-to-distortion ratio. It is assumed that only strong signals are to be penalized. Since the "ideal" signal-to-noise curve

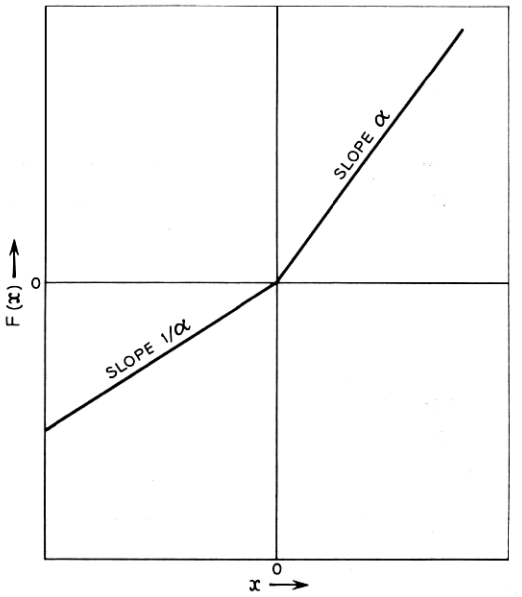

Fig. 2 — System transmission characteristic with a shift ϵ in the coder reference. Quantization is neglected.

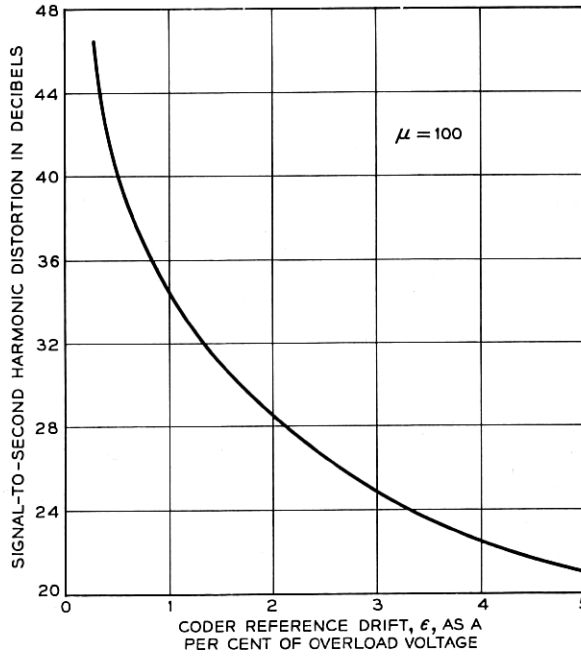

Fig. 3 — Plot of signal-to-second harmonic distortion as a function of coder reference shift expressed as a per cent of full load.

of Fig. 1 is approximately 34 db near full load, then using power law addition a $|S/D|$ of about 40 db is required to meet the 1-db margin. From Fig. 3 the 40-db figure implies a $\frac{1}{2}$ per cent tolerance on the coder dc shift.

2.3 *Signal-to-Noise Behavior of the Experimental Terminal*

A series of tests was performed to evaluate the degree to which the previous assumptions and calculations describe the laboratory model. In all cases, tests were made with sinusoids to permit probing the largest quantizing steps of the companded-coding system without the difficulty of peak clipping.

The signal-to-noise ratio was measured with an instrument which compares the average power of signal plus noise to the average power of the noise including distortion products. No measurements were made which allowed separation of the total noise into its components. The noise was determined by removing the signal with a narrow-band rejection filter. Both indications are calibrated to read rms for sinusoidal

signals. With the signal-to-noise ratios of interest, no special problem exists in establishing the output signal power in this manner. Careful checks indicate that errors of up to 1 db are possible for low-level signals. Fig. 4 shows the signal-to-noise ratio as a function of signal level for the extreme channels and the mean curve for 24 channels. The measurements were made with no attempt to optimize individual channels. Channel-to-channel variation is attributed primarily to pedestal variation prior to compression and dc shifts in the encoder reference. The curve corresponding to the previously stated objective is also shown.* Adequate performance is indicated.†

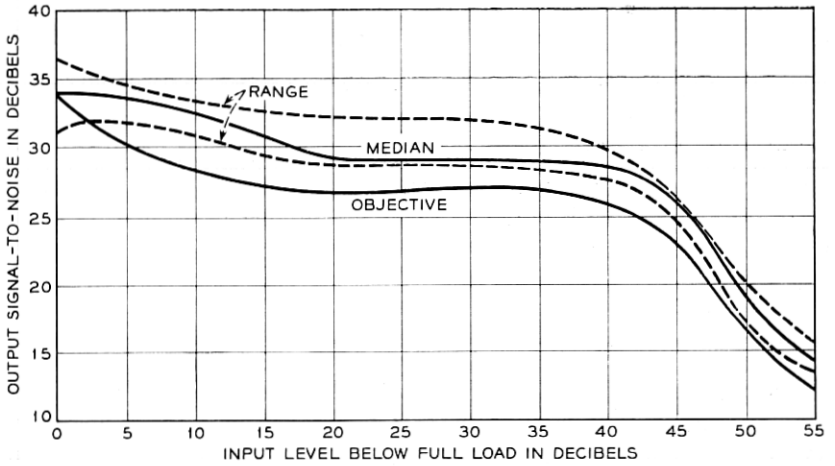

Fig. 4 — Plot of signal-to-noise measurements over 24 channels.

When sinusoidal modulating signals are used for system testing, variation in signal-to-noise as a function of the excitation frequency is to be expected.[3] When the frequency is small in relation to the sampling frequency, approximately the same performance is obtained for both sine waves and speech. As the frequency is increased, quantizing impairment is reduced. This is illustrated by the signal-to-noise measurements of Fig. 5. A constant input level is used for these measurements. The channel bandpass characteristics are given in Fig. 6 to explain the signal-to-noise falloff above 2600 cycles.

* This curve is obtained by reducing the signal-to-noise ratio by 3 db at all points on the curve for the actual compandor in Fig. 11 of Ref. 1.

† These results do not display common equipment variations contributing to system-to-system differences.

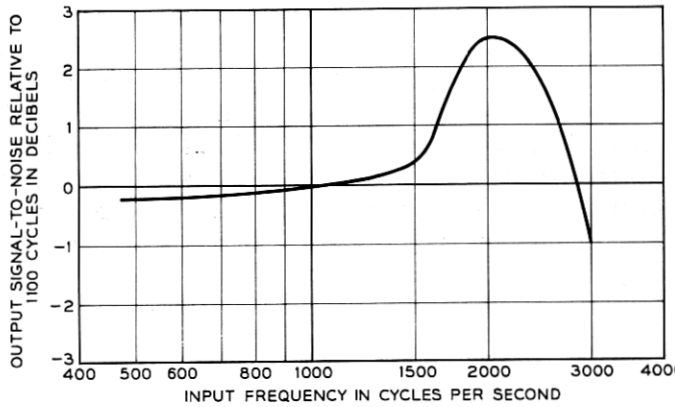

Fig. 5 — Plot of signal-to-noise ratio vs input frequency.

Submultiples of the sampling frequency were avoided in the measurements because at such points harmonics of the input signal produced by quantization beat with harmonics of the sampling frequency. For this reason, the measurements described previously were made with an 1100-cycle tone.

III. IDLE CIRCUIT NOISE AND INTERCHANNEL CROSSTALK

As a result of pedestal variation, PCM channels in the absence of speech modulation exhibit an important enhancement of weak interference. Both noise and interchannel crosstalk are affected. The en-

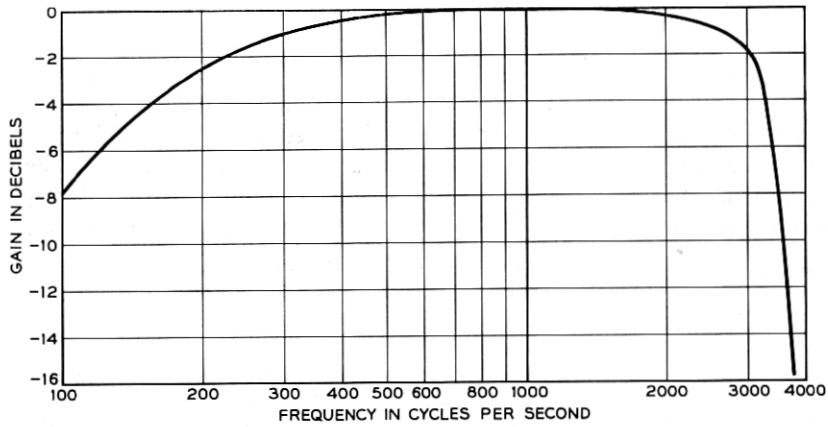

Fig. 6 — Typical bandpass characteristic of the channels.

hancement varies with pedestal drift and input interference, but is most pronounced when a quiescent channel is biased at the boundary between two adjacent quantizing steps or "mid-riser." Under this condition, any minute interference changes the quantized output and considerable enhancement is possible. In the following, a calculation of the interference power resulting at the system output under idle circuit conditions is presented. In addition, a series of noise and crosstalk measurements made on the experimental terminal are discussed.

3.1 *Analysis*

As a starting point for the analysis, it is assumed that noise and crosstalk are introduced into an idle channel prior to compression. The transmission characteristic between compressor and expandor is then derived, and the power spectrum of the interference at the expandor output is calculated. Finally, the noise and crosstalk spectrum components of interest are modified by the response of the system output filter and performance evaluated.

3.1.1 *Small-Signal Compressor-Expandor Transmission Characteristic*

With logarithmic companding and a perfect quantizer, the transmission characteristic between compressor input and expandor output is shown in Fig. 7. As indicated in the figure, the intermediate quantizer characteristic is decomposed into the sum of a linear term and a periodic sawtooth function for analytical convenience. This model for the staircase transducer was suggested by S. O. Rice and discussed in an earlier paper by W. R. Bennett.[4] The individual network characteristics can therefore be expressed as follows:

$$\begin{aligned}
&\text{Compressor:} \begin{cases} Y = \dfrac{V_0 \log\left(1 + \mu \dfrac{X}{V_0}\right)}{\log(1+\mu)} & (0 \leqq X \leqq V_0) \\ Y = \dfrac{-V_0 \log\left(1 - \mu \dfrac{X}{V_0}\right)}{\log(1+\mu)} & (-V_0 \leqq X \leqq 0) \end{cases} \\
&\text{Quantizer:} \quad Z = Y + \frac{V}{\pi} \sum_{n=1}^{\infty} \frac{(-1)^n}{n} \sin \frac{2\pi n Y}{V} \quad (-V_0 \leqq Y \leqq V_0) \\
&\text{Expandor:} \begin{cases} W = \dfrac{V_0}{\mu} (e^{Z/V_0 \log(1+\mu)} - 1) & (0 \leqq Z \leqq V_0) \\ W = \dfrac{-V_0}{\mu} (e^{-Z/V_0 \log(1+\mu)} - 1) & (-V_0 \leqq Z \leqq 0). \end{cases}
\end{aligned} \tag{3}$$

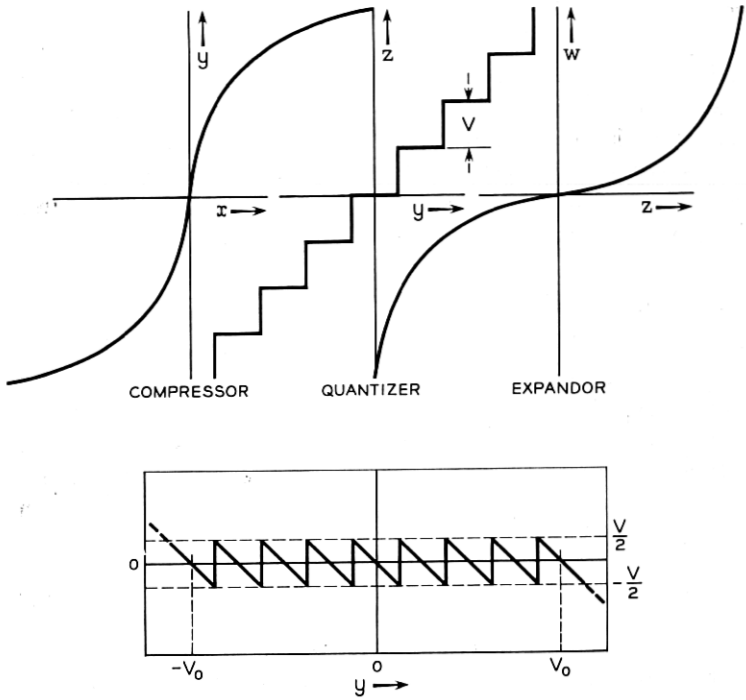

Fig. 7 — Transmission characteristics of the compressor, quantizer, and expandor. The quantizer transmission is decomposed into the sum of a linear term plus a periodic sawtooth function.

In these expressions V_0 is the system overload voltage, μ the compression parameter, and V the quantizer step size.

For a sufficiently small interference at the compressor input riding on a dc pedestal X_0, we can expand Y in a power series in the neighborhood of X_0, retaining only the first two terms. For positive X, therefore

$$Y \sim Y_0 + G(X - X_0) \tag{4}$$

where

$$Y_0 = \frac{V_0 \log\left(1 + \mu \frac{X_0}{V_0}\right)}{\log (1 + \mu)}$$

is the dc level at the quantizer input and

$$G = \frac{\mu}{\log (1 + \mu)} \cdot \frac{1}{1 + \mu \frac{X_0}{V_0}}$$

is the compressor small-signal gain.

Similarly, since the quantizer ac output will also be relatively small, and assuming that the operating point Z_0 at the expandor input is approximately Y_0,* then the expandor transmission can be written as

$$W \sim \frac{V_0}{\mu}\left(e^{Y_0/V_0 \log(1+\mu)} - 1\right) + \frac{\log(1+\mu)}{\mu} e^{Y_0/V_0 \log(1+\mu)}(Z - Y_0) \quad (5)$$

or substituting for Y_0 from above

$$W \sim X_0 + \frac{1}{G}(Z - Y_0).$$

Therefore, using the functional dependence of Z on Y as given by (3) and combining it with (4), W as a function of X becomes

$$W \sim X_0 + (X - X_0) + \frac{V}{G}\frac{1}{\pi}\sum_{n=1}^{\infty}\frac{(-1)^n}{n}\sin\left[\frac{2\pi n}{\frac{V}{G}}\left((X - X_0) + \frac{Y_0}{G}\right)\right]. \quad (6)$$

The input X consists of the idle channel interference (noise and crosstalk) plus the dc pedestal X_0. Therefore, $X' = X - X_0$ is the interference alone. If we denote Y_0/G by X_0' and V/G by V', then W may be written as

$$W \sim (X_0 - X_0') + (X' + X_0') + \frac{V'}{\pi}\sum_{n=1}^{\infty}\frac{(-1)^n}{n}\sin\frac{2\pi n}{V'}(X' + X_0'). \quad (7)$$

Neglecting $X_0 - X_0'$, which only produces a dc component at the output, W as a function of $X' + X_0'$ is given by

$$W \sim (X' + X_0') + \frac{V'}{\pi}\sum_{n=1}^{\infty}\frac{(-1)}{n}\sin\frac{2\pi n}{V'}(X' + X_0'). \quad (8)$$

This result is shown in Fig. 8 and is the small-signal transmission characteristic. The quantity X_0' gives the shift in reference produced by the dc pedestal X_0, and V' is the original quantizer step size reduced by the gain factor G. Since G varies inversely with X_0, then V' becomes larger as X_0 and thus X_0' are increased.

3.1.2 *Power Spectrum of the Interference at the Expandor Output*

The expandor output spectrum can be obtained from the statistical properties of the train of interference samples obtained at this point.

* This neglects dc shift as a result of quantization.

Assuming unit impulse sampling, the output spectrum is given by[5]

$$P(f) = \frac{1}{T}\sum_{k=-\infty}^{k=\infty} \psi_W(kT)e^{i2\pi f\,kT} = \frac{1}{T}\left[\psi_W(0) + 2\sum_{k=1}^{\infty}\psi_W(kT)\cos 2\pi f\,kT\right] \tag{9}$$

where T is the reciprocal of the sampling frequency f_s, and $\psi_W(kT)$ is the autocorrelation function at the expandor output evaluated at the sampling instants kT. This function can be determined directly from (8). Assuming $X'(t) = n(t) + E \sin 2\pi f_0 t$, where $n(t)$ is the input noise and the sinusoid represents crosstalk, then

$$W(t) = n(t) + E\sin 2\pi f_0 t + X_0' + \frac{V'}{\pi}\sum_{n=1}^{\infty}\frac{(-1)^n}{n}\sin\left\{\frac{2\pi n}{V'}\,(n(t) + E\sin 2\pi f_0 t + X_0')\right\}. \tag{10}$$

Using this result, $\psi_W(kT)$ is calculated by definition:

$$\psi_W(kT) = \langle W(t)W(t + kT)\rangle$$

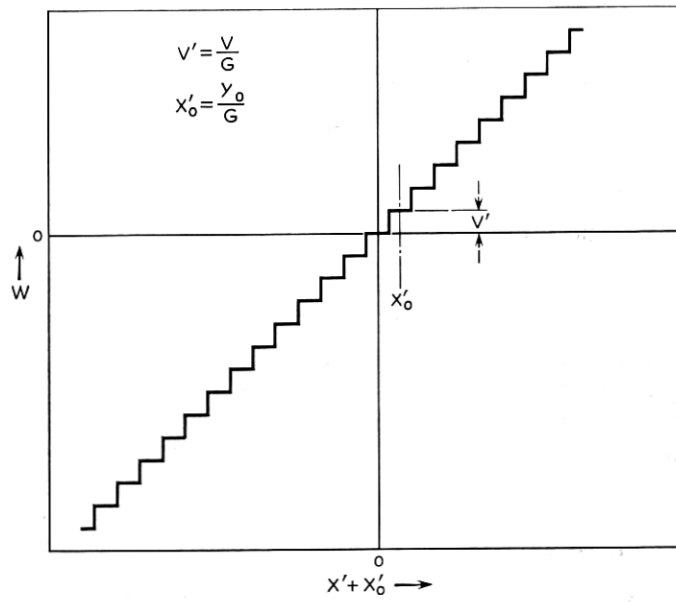

Fig. 8 — Small-signal transmission characteristic between compressor input and expandor output. The quantity X_0' gives the shift in reference produced by a dc pedestal at the compressor input.

where $\langle\ \rangle$ denotes expected value. If the input variables are all independent, the calculation of the autocorrelation function, although tedious, presents no formal difficulties. For the terms in the computation involving averages over the noise $n(t)$, a Gaussian amplitude distribution is assumed. This involves the autocorrelation of the input noise φ_{kT}, which is given by

$$\varphi_{kT} = \varphi_0 \frac{\sin \pi k}{\pi k} = \begin{cases} \varphi_0 & \text{for } k = 0 \\ 0 & \text{otherwise} \end{cases} \tag{11}$$

for a uniform noise spectrum over the voice band $(-f_s/2, f_s/2)$. The input noise power is φ_0. Under these conditions, (12) for $\psi_W(kT)$ is obtained. The J's in this expression are Bessel functions of the first kind. This result is used in (9) to determine the spectral components of noise and crosstalk.

$$\begin{aligned}
\psi_W(kT) = {} & \varphi_{kT}\left(1 + 4\sum_{n=1}^{\infty}(-1)^n J_0\left(\frac{2\pi nE}{V'}\right)\cos\frac{2\pi nX_0'}{V'}\, e^{-2(n\pi)^2\varphi_0/V'^2}\right) \\
& + \left(\frac{E^2}{2} + 2EV'\sum_{n=1}^{\infty}\frac{(-1)^n}{n\pi}J_1\left(\frac{2\pi nE}{V'}\right)\cos\frac{2\pi nX_0'}{V'}\, e^{-2(n\pi)_2\varphi_0/V'^2}\right) \\
& \cdot\cos 2\pi f_0 kT + \left(X_0'^2 + 2X_0'V'\sum_{n=1}^{\infty}\frac{(-1)^n}{n\pi}J_0\left(\frac{2\pi nE}{V'}\right)\sin\frac{2\pi nX_0'}{V'}\right. \\
& \left.\cdot e^{-2(n\pi)^2\varphi_0/V'^2}\right) + \sum_{n=1}^{\infty}\sum_{m=1}^{\infty}\frac{V'^2}{\pi^2}\frac{(-1)^{m+n}}{mn}\, e^{-2(m^2+n^2)\pi^2\varphi_0/V'^2} \\
& \cdot\left[\cos\frac{2\pi(m-n)X_0'}{V'}\, e^{4mn\pi^2\varphi_{kT}/V'^2}\left(\tfrac{1}{2}J_0\left(\frac{2\pi nE}{V'}\right)J_0\left(\frac{2\pi mE}{V'}\right)\right.\right. \\
& \left. + \sum_{l=1}^{\infty}J_l\left(\frac{2\pi nE}{V'}\right)J_l\left(\frac{2\pi mE}{V'}\right)\cos 2\pi l f_0 kT\right) + \cos\frac{2\pi(m+n)X_0'}{V'} \\
& \cdot e^{-4mn\pi^2\varphi_{kT}/V'^2}\left(\sum_{l=0}^{\infty}J_{2l+1}\left(\frac{2\pi nE}{V'}\right)J_{2l+1}\left(\frac{2\pi mE}{V'}\right)\cos 2\pi(2l+1)f_0 kT\right. \\
& - \tfrac{1}{2}J_0\left(\frac{2\pi nE}{V'}\right)J_0\left(\frac{2\pi mE}{V'}\right) - \sum_{l=1}^{\infty}J_{2l}\left(\frac{2\pi nE}{V'}\right)J_{2l}\left(\frac{2\pi mE}{V'}\right) \\
& \left.\left.\cdot\cos 2\pi(2l) f_0 kT\right)\right].
\end{aligned} \tag{12}$$

3.1.3 *System Output Power*

To determine the system output power, the expandor output spectrum, obtained from (9) and (12), is modified by the response of a channel filter. At the filter output we are interested in the following quantities.

(1) Total voice band noise power in the continuous spectrum in the absence of an input crosstalk signal.

(2) Total crosstalk power at the frequency f_0 with noise masking.*

Assuming that the output filter is flat over the voice band, has no dc transmission, and cuts off sharply at f_s, then the noise and crosstalk powers of interest become

$$N = \frac{1}{T^2}\left[\varphi_0\left(1 + 4\sum_{n=1}^{\infty}(-1)^n \cos\frac{2\pi n X_0'}{V'}\, e^{-2(n\pi)^2\varphi_0/V'^2}\right)\right]$$
$$+ \frac{1}{T^2}\left[\frac{V'^2}{2\pi^2}\sum_{n=1}^{\infty}\sum_{m=1}^{\infty}\frac{(-1)^{m+n}}{mn}\left(\cos\frac{2\pi(m-n)X_0'}{V'}\, e^{-2(m-n)^2\pi^2\varphi_0/V'^2}\right.\right.$$
$$\left.\left. - \cos\frac{2\pi(m+n)X_0'}{V'}\, e^{-2(m+n)^2\pi^2\varphi_0/V'^2}\right)\right] \qquad (13)$$
$$- \frac{1}{T^2}\left[\frac{V'^2}{\pi}\sum_{n=1}^{\infty}\sum_{m=1}^{\infty}\frac{(-1)^{m+n}}{mn}\, e^{-2(m^2+n^2)\pi^2\varphi_0/V'^2}\right.$$
$$\left.\cdot\sin\frac{2\pi n X_0'}{V'}\sin\frac{2\pi m X_0'}{V'}\right]$$

$$\overline{X} = \frac{1}{2T^2}\left[E + \frac{2V'}{\pi}\sum_{n=1}^{\infty}\frac{(-1)^n}{n}J_1\left(\frac{2\pi nE}{V'}\right)\cos\frac{2\pi n X_0'}{V'}\,\frac{e^{-2(n\pi)^2\varphi_0}}{V'^2}\right]^2. \qquad (14)$$

These expressions are evaluated in the following sections.

3.1.4 *Idle Circuit Noise*

Using the above result for N, curves of N vs X_0' with φ_0/V'^2 as a parameter can be plotted as shown in Fig. 9. The constant $1/T^2$ is omitted. In calculating these results, it is assumed that when X_0 varies such that X_0' moves between two adjacent decisions levels of Fig. 8, the step size V' remains constant.† That constant is determined by the value of X_0 which places the input X' at the midpoint of one of the input step intervals. Hence if $X_0' = \bar{m}V'$, for $\bar{m} = 0, 1, 2, 3, \cdots$ then

$$\bar{m} = \frac{V_0}{V}\,\frac{\log\left(1 + \mu\dfrac{X_0}{V_0}\right)}{\log(1+\mu)}$$

and solving the above for X_0 in terms of $\bar{m}$

* The output power at f_0 is a measure of the intelligible crosstalk interference.

† This approximation is valid for a small range of variation since the slope G of the compressor characteristic does not change materially for a small change in X_0.

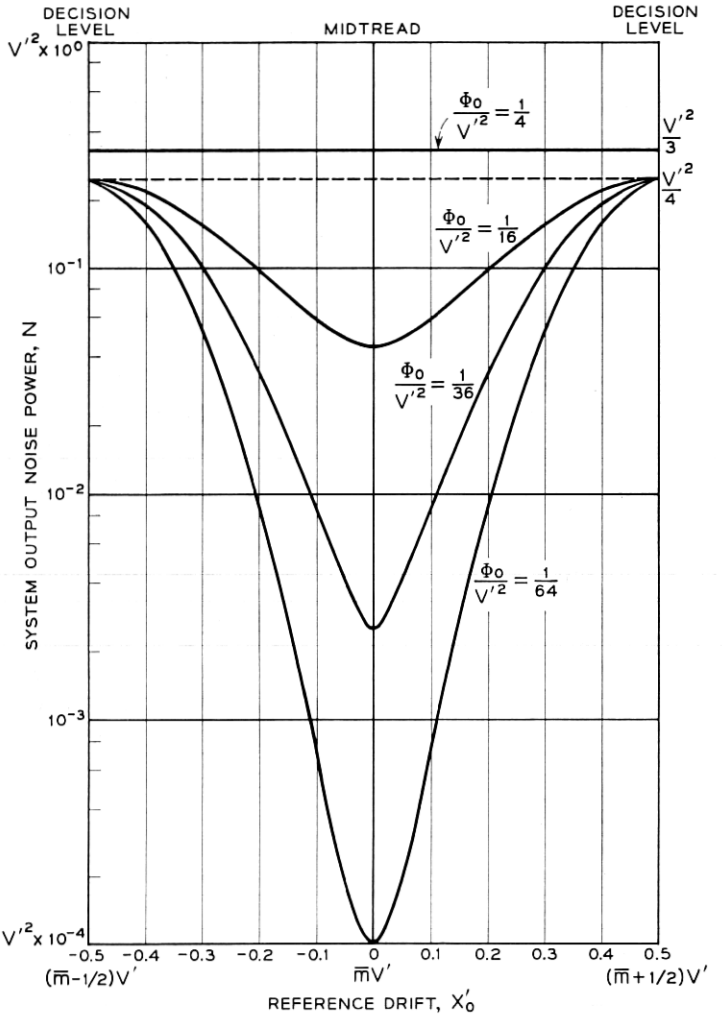

Fig. 9 — System output noise power vs reference drift X_0. The input noise power as a fraction of the step size V' is taken as a parameter. The reference drift is shown to vary between any two adjacent decision levels.

$$V' = \frac{V}{G} = V \frac{\log (1 + \mu)}{\mu} \exp \left\{ \bar{m} \frac{V}{V_0} \log (1 + \mu) \right\}. \qquad (15)$$

This result determines the value of V' to be used in Fig. 9 for any dc pedestal X_0 and thus $\bar{m}$.

With the above conditions in mind, the results of Fig. 9 are interpreted. First for φ_0/V'^2 sufficiently large, N becomes independent of

X_0'. The curve with $\varphi_0/V'^2 = 1/4$ is representative of this case and follows directly from (13). For example, the contribution of the summation appearing in the first bracketed term of this equation approaches zero under this condition, and the only contribution of any importance in the second and third terms is that for $n = m$. Therefore N reduces to the approximate expression

$$N \sim \frac{1}{T^2}\left[\varphi_0 + \frac{V'^2}{2\pi^2}\sum_{n=1}^{\infty}\frac{1}{n^2}\right] = \frac{V'^2}{T^2}\left[\frac{\varphi_0}{V'^2} + \frac{1}{12}\right] = \frac{V'^2}{3T^2} \qquad \left(\frac{\varphi_0}{V'^2} = \frac{1}{4}\right). \tag{16}$$

Hence, in this case, the output noise consists of the input noise plus a quantizing noise term in accord with Bennett's analysis.[4]*

When the input noise becomes smaller, the largest output power occurs for $X_0' = (m \pm \frac{1}{2})V'$ or the reference at "mid-riser" (quantizer decision level). In this situation the output is independent of the input when the latter is sufficiently small. Under this condition, the quantizer of Fig. 8 puts out a square wave with ac swing V' and random zero crossings. This results in a lower limit beyond which the system output noise power cannot be reduced. This lower limit is $V'^2/4$ and is called the noise "floor." As the dc pedestal becomes larger, V' and the "floor" become higher. This is a worst-case situation and occurs only for "mid-riser" biasing. As indicated in Fig. 9, performance improves as the reference departs from this location.

3.1.5 *Interchannel Crosstalk*

In evaluating crosstalk performance from the expression for $\overline{\underline{X}}$ in (14), we consider only the "mid-riser" condition or $X_0' = (m \pm \frac{1}{2})V'$ for $\bar{m} = 0, 1, 2, 3, \cdots$. This yields the worst possible crosstalk performance for weak input crosstalk signals. Hence $\overline{\underline{X}}$ becomes

$$\overline{\underline{X}} = \frac{1}{2T^2}\left[E + \frac{2V'}{\pi}\sum_{n=1}^{\infty}\frac{1}{n}J_1\left(\frac{2\pi nE}{V'}\right)\exp - \left(\frac{2(n\pi)^2\varphi_0}{V'^2}\right)\right]^2. \tag{17}$$

This result is plotted in Fig. 10 as a function of input crosstalk power with φ_0/V'^2 as a parameter. As before, $1/T^2$ is omitted, and it is assumed that E/V' is <1 so that the input crosstalk signal is confined to one step. V' is related to V by (15).

The results of Fig. 10 parallel those of Fig. 9 very closely. For example

* Since $V' = V/G$, where $1/G$ is the expandor small signal gain, then the term $V'^2/12$ also illustrates companding improvement as a function of dc pedestal X_0 as discussed by Smith in Ref. 2.

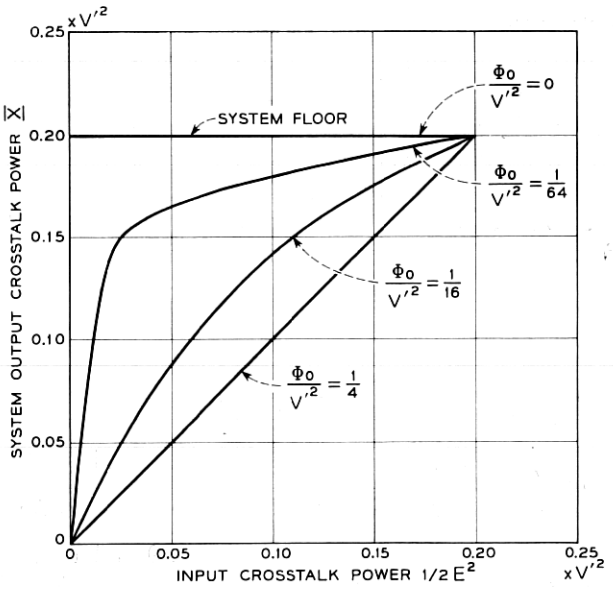

Fig. 10 — System output crosstalk power vs input crosstalk power with the input noise power as a fraction of the step size V' taken as a parameter. The quantizer reference is assumed to be at a decision level for purposes of determining this set of curves.

with φ_0/V'^2 sufficiently large ($\varphi_0/V'^2 = 1/4$), $\bar{X}$ becomes $E^2/2T^2$. In other words, the system transmits the input crosstalk signal without enhancement. Qualitatively, when the input crosstalk is sinusoidal, background noise tends to scramble its zero crossings, thus producing a width modulation in the output square wave. The net result is linear transmission at f_0, the frequency of the input, provided the noise masking is large enough.

For other values of input noise, a nonlinear input-output power relationship exists. In the special case $\varphi_0/V'^2 = 0$, $\underline{\bar{X}}$ reduces to

$$1/2T^2(2V'/\pi)^2.$$

This corresponds to the power in the fundamental of an output square wave with unperturbed zero crossings. The system output crosstalk power that exists under these conditions is called the crosstalk "floor," and is the minimum power output when the bias is at "mid-riser." As in the case of idle circuit noise, the crosstalk "floor" depends directly on V', and is therefore higher as the dc pedestal becomes larger.

3.1.6 *System Performance*

In this section, performance is put in numerical terms by using the parameters of the experimental system. The parameters of interest are: (1) 7-digit encoding (128 quantizing levels), (2) 26-db companding ($\mu = 100$), (3) clipping level or overload point defined by a +3-dbm sine wave at the system input (0-db TL) and (4) 2-db net loss from system input to output. Using (1) through (4), the following relationships can be inferred

$$\frac{V_0}{V} = 64$$

$$G\Big|_{x_0 \to 0} = 20 \log_{10} \frac{\mu}{\log (1 + \mu)}\Big|_{\mu=100} = 26 \text{ db}$$

$$10 \log_{10} \frac{V_0^2}{2} = \begin{cases} +3 \text{ dbm at 0-db TL (system input)} \\ +1 \text{ dbm at } -2\text{-db TL (system output)}. \end{cases}$$

These numbers, used in conjunction with Figs. 9 and 10, are sufficient information to evaluate system performance with any dc pedestal X_0. A worst-case situation exists when the dc reference for the interference is at a decision level. The performance obtained under this condition will therefore be considered exclusively in what follows.

First, it is assumed that the dc pedestal is sufficiently small so that $X_0 = V'/2$ and $V' = V[\log (1 + \mu)/\mu]$ for $\bar{m} = 0$, as given by (15). In this case the system noise "floor" is 18 dba at the -2TL with F1A line weighting,* and the crosstalk "floor" at this same point is -65 dbm. The output noise power of 18 dba is the minimum obtainable when the reference shifts to the first decision level. This then is a fundamental system limitation. On the other hand, the crosstalk "floor" exists only without the masking effect of background noise. The improvement obtained with noise masking is related in a nonlinear fashion to the mean square noise at the compressor input as indicated in Fig. 10. With 20 dba of input noise referred to the 0-db TL ($\varphi_0/V'^2 = 1/4$), no crosstalk enhancement occurs, and the system output crosstalk power is linearly related by the system net loss to the input power at the 0-db TL.

For a larger dc pedestal, V' is increased and the system noise and crosstalk "floors" are higher. The degradation in system performance is determined directly from (15) and is given by $20 \log_{10} (1 + \mu X_0/V_0)$ db. It should be pointed out that this same factor is involved in deter-

* Using F1A line weighting, "white" noise in a 3-kc band at 0 dbm corresponds to 82 dba.

mining the amount of noise masking required to achieve a given improvement over the crosstalk "floor". For example, for a larger value of V' the input noise power φ_0 must also be larger in order to maintain φ_0/V'^2 constant and hence the same masking ratio.

The effect of a larger dc pedestal, as illustrated above, is essentially the same as the loss in companding improvement from this same cause, as discussed by Smith. Therefore, as mentioned in Section 2.2, the effect is not as pronounced in the experimental system as one would predict from "ideal" logarithmic companding when the factor $(1 + \mu X_0/V_0)$ applies.*

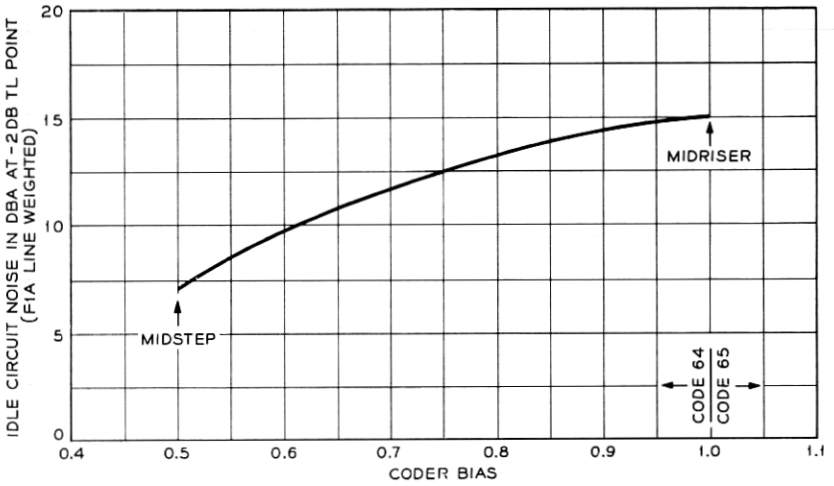

Fig. 11 — Measured output noise power vs coder reference drift in the range between codes 64 and 65. All measurements are in dba and are referred to the −2-db TL point.

3.2 *Measured Noise Performance*

All evaluations of the output idle circuit noise were made with a 2B noise meter using F1A line weighting. In all cases, the other end of each trunk was terminated in 900 ohms + 2μf, the nominal terminating impedance of the trunks. Variations of noise as a function of the bias position on the coder step are shown in Fig. 11 with variations from 7 to 15 dba. All measurements are at the −2-db TL point.

The general flattening of the experimental curve of Fig. 11 could be attributed to a substantial input noise at the compressor referring to

* For $X_0/V_0 = 1\%$, $(1 + \mu X_0/V_0)$ yields a 6-db degradation. The loss in companding improvement for a 1 per cent pedestal is only about 2 db in the experimental system so that the noise and crosstalk "floors" would only be 2-db higher.

TABLE I — IDLE CIRCUIT NOISE IN DBA AT −2-db TL

Channel Number	DBA	Channel Number	DBA
1	11.0	13	7.0
2	11.0	14	6.0
3	12.0	15	11.0
4	11.5	16	14.0
5	10.5	17	11.0
6	15.0	18	11.0
7	6.0	19	12.0
8	14.0	20	13.5
9	11.0	21	14.0
10	10.5	22	13.5
11	14.0	23	11.0
12	13.0	24	11.0

the curves of Fig. 9. Also, when the coder is adjusted for the decision-level bias position, some variation in bias occurs, so that the output power at this point tends to be an average over a range of bias. For this reason, the 15-dba measured noise floor is lower than the calculated value of 18 dba. Table I gives a typical distribution of noise measured on all 24 channels with no special care being taken to optimize each.

The total range 6 to 15 dba is explained by Fig. 11 with the distribution fairly uniform between these extremes. The mean value in dba is 11.4, which would be expected from a large number of channels uniformly distributed in bias if Fig. 11 were a linear plot.

3.3 *Measured Crosstalk Performance*

To obtain realistic results, all crosstalk evaluation was made with 15 dba (F1A weighted) of noise applied to the input of the trunks under test. The crosstalking channel was supplied with a 0-dbm sinusoid (at the 0-db TL point) at a frequency of 1100 cycles.

Fig. 12 shows the results of measurements of crosstalk of each channel into every other channel. The only pattern of significance in these data is that of a minimum of crosstalk among channels in the same compressor. Earlier descriptions of the dual compressor plan by Davis[6] have explained the grouping of all even-numbered channels in one compressor and odd in a second. The best crosstalk performance between channels in the same compressor is in the range of −72 to −75 dbm, whereas for channels in the other compressor the range is −73 to −80 dbm. This is a clear indication of transmitter terminal crosstalk.

Extensive measurements have not been made of crosstalk in the absence of intentionally introduced random noise in the channel being measured; however, sample tests show that crosstalk varied up to 6 db

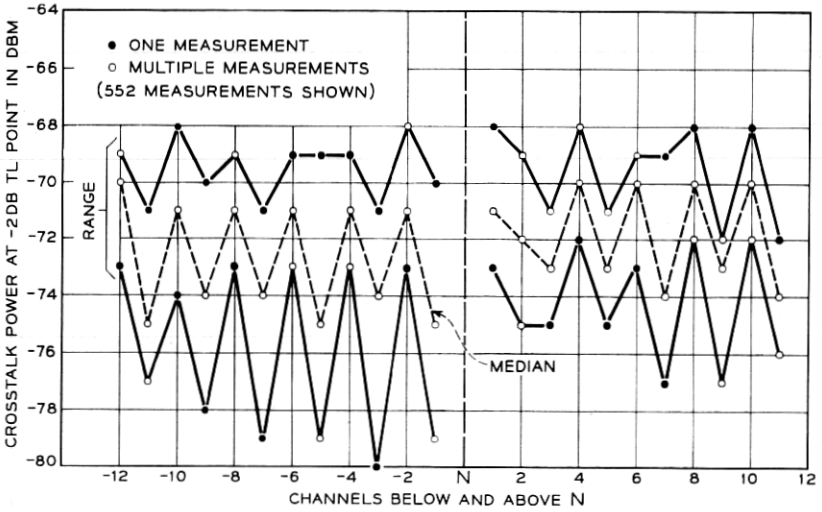

Fig. 12 — Measured output crosstalk power in the $(N + K)$th channel due to a tone in the Nth. All measurements are referred to the −2-db TL point.

with and without noise added. The crosstalk enhancement is in practice never infinite, even with the analog crosstalk small compared to one coder step, because the system is not noise-free. At the input to the compressor, the inband rms value of random noise was approximately $\frac{1}{6}$ of a code step during normal operation.

IV. NET LOSS INSTABILITY AND GRANULARITY

The control and measurement of net loss presents two major problems in the system. The first is the enhancement of variations in linear gain occurring between compressor input and expandor output. The second is a result of the encoding process which introduces granularity in the system response to a transmitted sine wave. The latter poses the problem of net loss measurement with a sinusoidal input, a standard testing procedure. Both of these effects are considered in the sections to follow. In addition, a gain variation margin assignment to the major blocks of the transmitting and receiving terminals is made. Finally, net loss measurements made on the terminals are presented.

4.1 *Linear Gain Variation Enhancement*

This effect can be analyzed by determining $G(x)$, the transmission characteristic provided by a back-to-back compressor-expandor com-

bination with an intermediate linear gain perturbation. Using the logarithmic compression curve given by (1) previously, multiplying the output y by $1 + \delta$, where δ is the linear gain variation, and feeding the result into the inverse expandor characteristic, the following expression is obtained for small δ.

$$\begin{aligned} G(x) &= x + \frac{\delta}{\mu}(1 + \mu x)\log(1 + \mu x) \qquad (0 \leqq x \leqq 1) \\ G(-x) &= -G(x). \end{aligned} \tag{18}$$

The first term gives the desired linear transmission and the second term the nonlinearity produced by δ.

The measurement of net loss is generally made with a sinusoidal input. Using the transmission characteristic given by $G(x)$, the recovered fundamental can be determined. This is accomplished by setting $x = E \sin wt$ and computing the fundamental component in the Fourier series at the output. In-band distortion produced by higher harmonics in the response is not considered. Under these conditions, the linear gain variation enhancement, i.e., the factor by which the gain is multiplied, is shown in Fig. 13. This curve gives the enhancement as a function of the amplitude E of the input sine wave normalized to the system overload voltage. Unity input corresponds to full load. The compression parameter μ is taken to be 100 in accordance with the laboratory design. The enhancement will be larger for a larger μ, however.

For signals considerably below full load the enhancement is small. This follows since compressor and expandor transmission are essentially linear in this range. At the other extreme, the enhancement takes on its maximum value and is approximately equal to the slope of the expandor characteristic at full load. This quantity is $\log(1 + \mu) = 4.6$ for $\mu = 100$ and indicates that a variation in linear gain is magnified 4.6 times for full-load signals. It is therefore apparent that considerably more control is required over deviations in linearity between compressor and expandor than for simple gain variations in other parts of the system.

4.2 *Net Loss Granularity*

Granularity of transmitted signal values for sinusoidal inputs is inherent in the PCM process. Measurement of system net loss with a sine wave, therefore, presents a problem independent of any circuit gain instability that may exist. The effect involved can be described by an

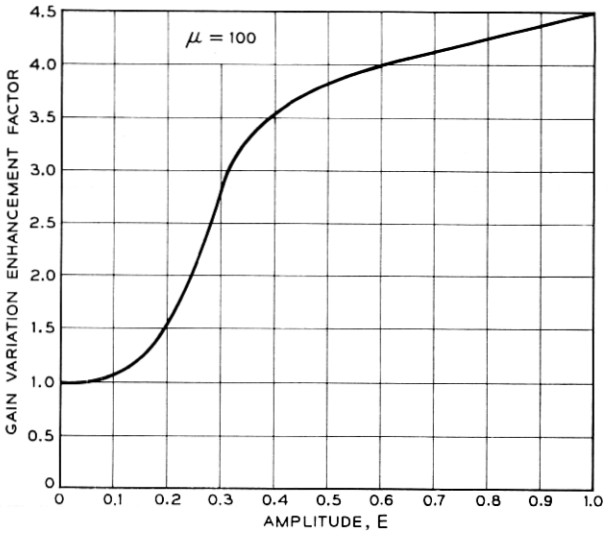

Fig. 13 — Gain variation enhancement factor as a function of the amplitude of the input sinusoid. Unity input corresponds to full load. The compression parameter μ is taken to be 100.

oscillatory gain curve as a function of the amplitude of the input sine wave. The extent of the gain variation is much greater for weak signals than for signals near full load due to quantization. However, values of the input signal may be found in any signal range for which the gain variation vanishes. To minimize the error in the testing procedure, therefore, test tones for net loss measurement should be confined to the vicinity of full load in the neighborhood of one of the nulls.

4.3 *Net Loss Objectives*

As noted earlier (Section 3.1.6), an objective of the experimental design was to provide a 2-db loss trunk. In this section a gain variation margin assignment is made to the major circuit blocks of the transmitting and receiving terminals. The allocation assumes that in the worst case an upper limit of 1.5 db variation from nominal is not to be exceeded. Therefore margins assigned to individual circuits are the maximum allowable assuming in-phase addition of effects from block-to-block.

The portions of the terminal equipment essential to this discussion are shown below with the margins assigned.

Transmitting Terminal	*Receiving Terminal*
Hybrid ± 0.05 db	Decoder ± 0.05 db
Filter and gate ± 0.1 db	Expandor network ± 0.45 db
Compressor preamp ± 0.1 db	Expandor postamp ± 0.1 db
Compressor network ± 0.45 db	Common amplifier ± 0.1 db
Compressor postamp ± 0.05 db	Gate and filter ± 0.1 db
Encoder ± 0.05 db	

The numbers in this table cannot be added directly to obtain the overall 1.5-db requirement. They have been determined so that ±0.55 db is allotted to those circuits which are physically outside of the path between compressor input and expandor output. The remaining ±0.95 db is proportioned among the remaining companding and encoding-decoding circuits. The latter allotment is higher to allow for enhancement effects introduced by the nonlinear transmission characteristics of the compressor and expandor networks.

As mentioned in Section 4.1, an enhancement factor of 4.6 for full-load signals applies when changes in linear gain between compressor and expandor networks occur. Therefore, the *linear* gain variation contributed by circuits located electrically between the compressor and expandor networks must be more accurately controlled. Included are the post-amplifier associated with the compressor network and the encoder and decoder. Allowing 0.5 db of the 0.95 db to this cause results in the 0.05 db allotment specified for each of these circuits. For the compressor and expandor networks themselves, we consider the gain variation produced by mistracking as discussed in Ref. 1. In view of these results, it would appear that the 0.45-db allocation is adequate.

4.4 *Net Loss Measurements*

Net loss measurements are made with an 1100-cycle 0-dbm tone at the 0-db TL. A full load sinusoid is +3 dbm at the 0-db TL. To illustrate the net loss as a function of signal level, the data shown in Fig. 14 were taken on the experimental terminal. The circuit transmission relative to that found for a 0-dbm tone is plotted. The relative measurement accuracy with the oscillator detector combination used for the measurements was approximately ± 0.05 db.

The large oscillations for weak signals show the granularity effect described previously. Fig. 14 shows the influence of a second phenomenon of approximate magnitude of 0.3 db. The broad slopes upon which the cyclic variations are superimposed are a result of compandor mistracking.

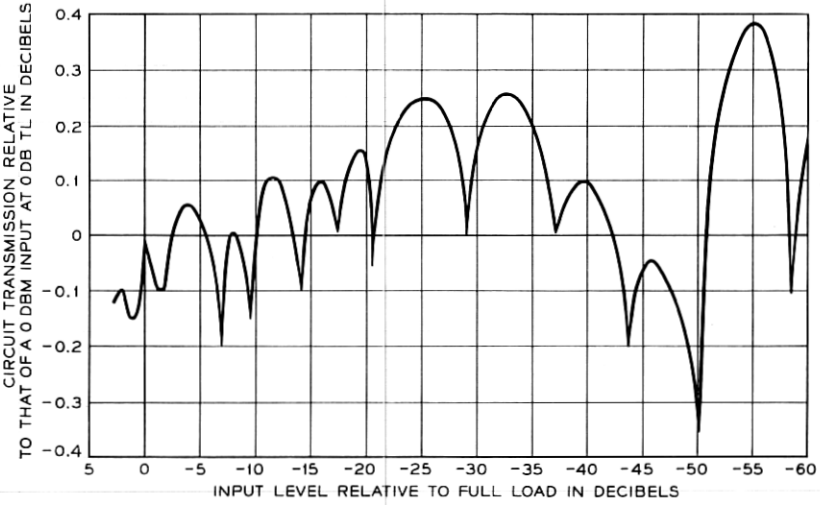

Fig. 14 — Net loss measurements — measured transmission relative to that for a 0-dbm input sinusoid.

V. LOAD CAPACITY

The overload performance of the system is determined primarily by clipping in the encoder-decoder combination. Neglecting quantization this can be represented ideally by the limiter characteristic of Fig. 15.* The following discussion is concerned with signal compression and harmonic distortion as a result of this limiting action. Measurements provided corroborate the analytical discussions.

5.1 *Sine Wave Response*

The system sine wave response is handled most conveniently using the integral representation given below for the characteristic of Fig. 15

$$H(x) = \frac{2}{\pi}\int_0^\infty \frac{\sin \mu \sin \mu x}{\mu^2}\, d\mu . \tag{19}$$

Denoting x by $E \sin wt$, the response becomes

$$H[E \sin wt] = \frac{4}{\pi}\sum_{n=0}^{\infty} I_{2n+1} \sin (2n+1)wt \tag{20}$$

* This neglects any shift in code scale introduced by the encoder. Since the latter is required to be small to reduce second-harmonic distortion as discussed earlier, its effect on overload performance is not considered.

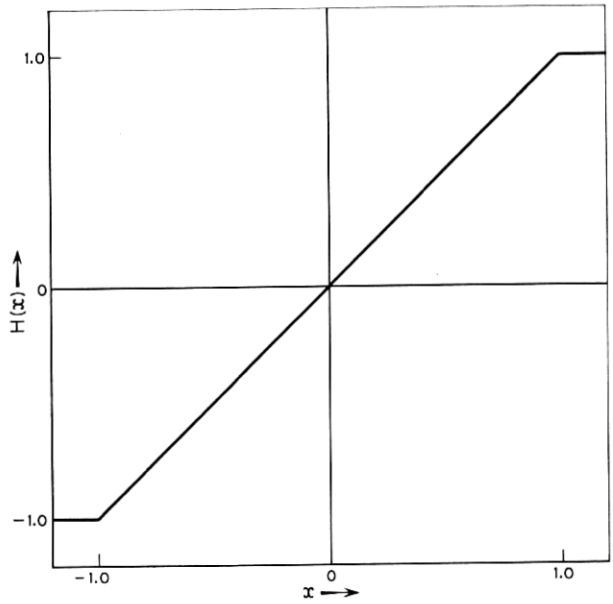

Fig. 15 — Limiting characteristic of system transmission in the absence of quantization.

where

$$I_{2n+1} = \int_0^\infty \frac{\sin \mu J_{2n+1}(\mu E)}{\mu^2}\, d\mu .$$

The J's in the preceding expression are Bessel functions of the first kind. Performing the required integration we get

$$I_1 = \frac{1}{2}\left[E \sin^{-1}\frac{1}{E} + \frac{\sqrt{E^2 - 1}}{E}\right] \qquad (n = 0)$$

$$I_{2n+1} = \frac{\sqrt{E^2 - 1}\, \sin\left[(2n+1)\sin^{-1}\dfrac{1}{E}\right]}{[(2n+1)^2 - 1]} - \frac{\cos\left[(2n+1)\sin^{-1}\dfrac{1}{E}\right]}{(2n+1)[(2n+1)^2 - 1]} \qquad (n > 0). \tag{21}$$

These results apply for signals above the clipping level or $E \geqq 1$, and give the harmonic content of the response. The first and third harmonics

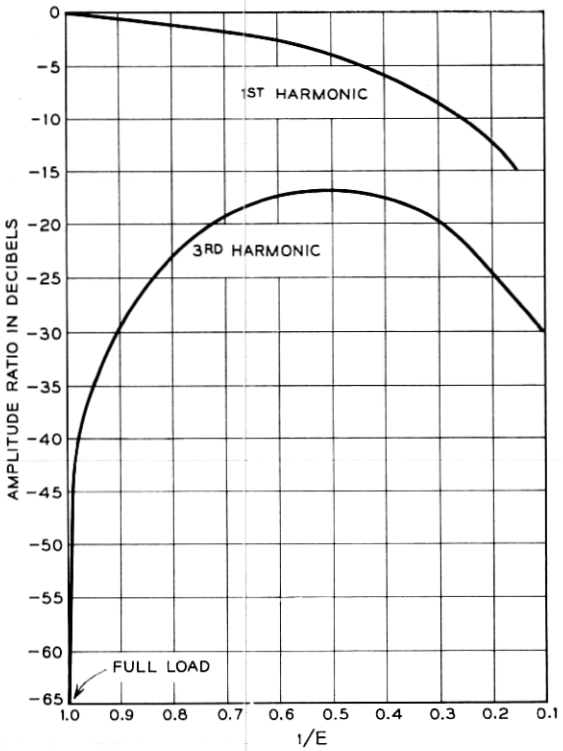

Fig. 16 — Plot of first and third harmonics of limiter response to a sinusoid.

relative to the input amplitude E are shown in Fig. 16 as a function of $1/E$.

5.2 *Measured Overload Performance*

The measured overload signal compression of the system is shown in Fig. 17. Calculated points extracted from the first harmonic response in Fig. 16 are also shown therein, indicating good agreement between calculation and experiment.

In addition to the response at the fundamental, harmonic distortion is also of interest. In this connection, the signal-to-noise ratio for signals above full load was measured. The measurement procedure was the same as indicated in Section 2.3. The results are shown in Fig. 18. Calculated results for the ratio of the first to third harmonic extracted from Fig. 2 are also shown at several points. Only points where clipping is

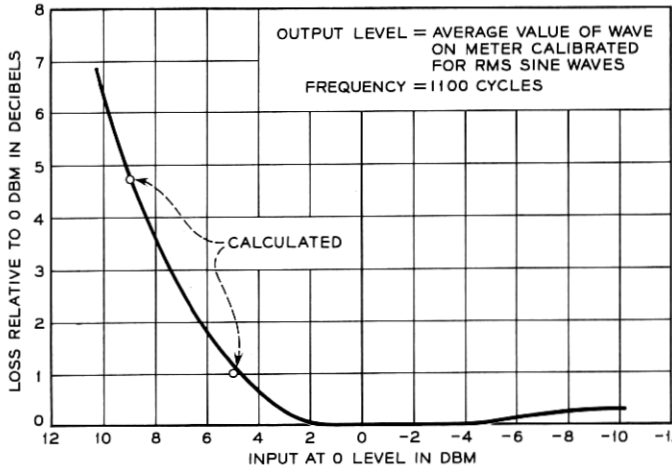

Fig. 17 — Measured signal compression vs input signal level.

appreciable are included, so that a valid comparison without quantizing impairment can be made. Agreement is good, thus indicating that only third harmonic distortion is appreciable.

VI. CONCLUSIONS

Four areas of system performance have been discussed. The measured performance has been compared with anticipated theoretical predictions. In all cases the system appears to be acceptable. No important or unex-

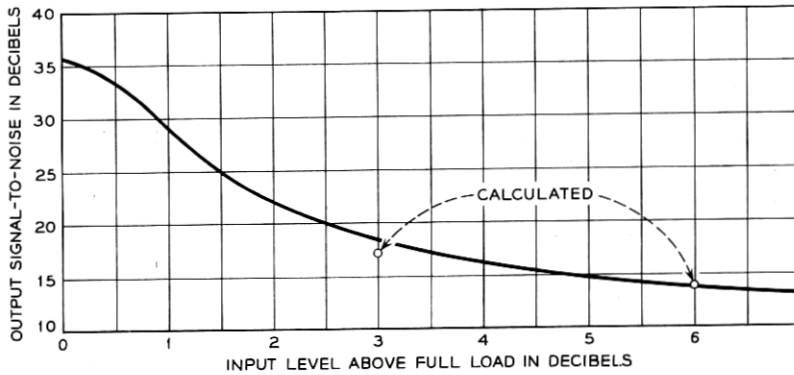

Fig. 18 — Measured signal-to-noise ratio vs input signal level for signals above full load.

plained differences between theoretical and actual performance have been discovered.

VII. ACKNOWLEDGMENTS

As in any corporate development, many members of Bell Laboratories have made significant contributions to the terminal design and evaluation programs. Particular mention should be made of the work of C. G. Davis on early phases of the system planning and functional arrangements, and of the work of D. J. Leonard in the design and execution of experiments for the system evaluation.

REFERENCES

1. Mann, H., Straube, H. M., and Villars, C. P., this issue p. 173.
2. Smith, B., B.S.T.J., **36,** May, 1957, p. 653.
3. Levin, G. A., and Golovichner, M. M., Radiotechnika SSRV V. **10,** No. 8, 1955, p. 3.
4. Bennett, W. R., B.S.T.J., **27,** July, 1948, p. 446.
5. Bennett, W. R., B.S.T.J., **37,** Nov., 1958, p. 1501.
6. Davis, C. G., this issue, p. 1.